

# Stability of Zn(II) Cations in Chabazite Studied by Periodical Density Functional Theory

Luis Antonio M. M. Barbosa\* and Rutger A. van Santen

Contribution from the Schuit Institute of Catalysis, Eindhoven University of Technology, P.O. Box 513, 5600 MB Eindhoven, The Netherlands

Jürgen Hafner

Institut für Materialphysik and Center for Computational Material Science, Universität Wien, Sensengrass 8, A-1090 Wien, Austria

Received June 19, 2000. Revised Manuscript Received January 29, 2001

**Abstract:** The location of the Zn<sup>2+</sup> cation in Zn-exchanged chabazite has been studied by the periodical density functional method. Chabazite was chosen as a zeolite model, because it contains three different types of rings commonly found in the zeolite structures: four-, six-, and eight-membered rings. Two aluminum atoms have been employed to substitute the silicon atoms in the same D6R unit cell of the zeolite framework. This leads to different arrangements for the Brønsted site pair and the Zn(II) cation. The two Brønsted sites are found to be more stable when placed in the small ring (4T ring) than in the other rings. This suggests that the most reactive Brønsted sites are located in the large rings. Two Brønsted sites are most stable when the O(H)–Al–O–Si–O(H)–Al sequence is followed in the same ring instead of being located in two different rings. This resembles the aluminum distribution in the small four-membered ring and agrees with bond order conservation rules. The cation stability is markedly influenced by the distortions of the framework. Other factors that also contribute to the stabilization are the aluminum content near the cation and the stability of the original Brønsted sites. The Zn<sup>2+</sup> cation is more stable in the large rings than in the small ones, the six-membered one being the most stable configuration. In the small rings, the cation is, therefore, more reactive. Two different probe molecules have been used to study the interaction with the Zn(II) cation: water and methane. These probe molecules can extract the active center from its original position. For the water molecule, this effect is large and leads to a high framework relaxation. The value of the binding energy of this molecule to the active sites is influenced by these framework relaxations as well as by the cationic position environment. For weakly interacting methane, these effects are significantly less.

## 1 Introduction

Zeolite catalysts are extensively used in petroleum refining as well as in the petrochemical and chemical industries. In many industrial processes zeolites are employed as a solid acidic catalyst. In recent years, a number of new processes have been developed, which are based on metal loaded zeolites. Aromatization of alkanes, which is well addressed in the literature,<sup>1,2,3,4</sup> is an example of a reaction of great economical interest. Especially Ga and Zn activated zeolites have been used to promote this reaction.<sup>1,4</sup>

Zeolites are also used for small molecules separation, such as air-separation.<sup>5</sup> Interaction with the cations plays a major role in such processes. Because N<sub>2</sub> has a higher affinity with cations than O<sub>2</sub> does, an oxygen-rich gas phase can be prepared by such materials.<sup>6</sup>

Many experimental studies have been directed to an understanding of the catalytic effect of these cationic species<sup>3,7–15</sup> as well as to determine their location in the zeolite micropores.<sup>16–33</sup> Others investigated molecular aspects of the interaction with

\* Corresponding author. Present address: Institute de Recherches sur la Catalyse, C.N.R.S., 2 Avenue Albert Einstein, Villeurbanne Cedex 69626, France. E-mail: lbarbosa@catalyse.univ-lyon1.fr.

(1) Ono, Y. *Catal. Rev. Sci. Eng.* **1992**, *34*, 179.  
 (2) Frash, M. V.; van Santen, R. A. *Phys. Chem. Chem. Phys.* **2000**, *2*, 1085.  
 (3) Biscardi, J. A.; Meitzner, G. D.; Iglesia, E. *J. Catal.* **1998**, *179*, 192.  
 (4) Kumar, N.; Lindfors, L.-E. *Catal. Lett.* **1996**, *38*, 239.  
 (5) Armor, J. N. *Microporous Mesoporous Mater.* **1998**, *22*, 451.  
 (6) Grey, T.; Gale, J.; Nicholson, D.; Peterson, B. *Microporous Mesoporous Mater.* **1999**, *31*, 45.

(7) de Lara, E. C.; Seloudoux, R. *J. Chem. Soc., Faraday Trans. 1* **1983**, *79*, 2271.  
 (8) Kazansky, V. B.; Kustov, L. M.; Khodakov, A. Y. *Zeolites: Facts, Figures, Future*, Jacobs, P. A., van Santen R. A. Eds., Elsevier Science Publishers: Amsterdam, 1989; p 1173.  
 (9) Kustov, L. M.; Kazansky, V. B. *J. Chem. Soc., Faraday Trans* **1991**, *87*, 2675.  
 (10) Khodakov, A. Y.; Kustov, L. M.; Kazansky, V. B.; William, C. J. *J. Chem. Soc., Faraday Trans* **1993**, *89*, 1393.  
 (11) Uvarova, E. B.; Kustov, L. M.; Lishchiner, I. I.; Malova, O. V.; Kazansky, V. B. *Stud. Surf. Sci. Catal.* **1997**, *105*, 1243.  
 (12) Kazansky, V. B.; Borovkov, V. Y.; Serykh, A. I.; van Santen, R. A.; Stobbelaar, P. J. *Phys. Chem. Chem. Phys.* **1999**, *1*, 2881.  
 (13) Yamazaki, T.; Abe, Y.; Watanuki, I.; Ozawa, S.; Ogino, Y. *Langmuir* **1988**, *4*, 433.  
 (14) Chen, L.; Lin, L.; Xu, Z.; Zhang, T.; Xin, Q.; Ying, P.; Li, G.; Li, C. *J. Catal.* **1996**, *161*, 107.  
 (15) Huber, S.; Knözinger, H. *Chem. Phys. Lett.* **1995**, *244*, 111.  
 (16) Calligaris, M.; Nardin, G.; Randaccio, L.; Comin, P.; Chiaramonti, *Acta Crystallogr.* **1982**, *B38*, 602.  
 (17) O'Connor, J. F.; Townsend, R. P. *Zeolites* **1985**, *5*, 158.  
 (18) Calligaris, M.; Mezzetti, A.; Nardin, G.; Randaccio, L. *Zeolites* **1985**, *5*, 317.  
 (19) Dutta, P. K.; Del Barco, B. J. *Phys. Chem.* **1985**, *89*, 1861.  
 (20) Dutta, P. K.; Shieh, D. C.; Puri, M. *Zeolites* **1988**, *8*, 306.  
 (21) Klier, K. *Langmuir* **1988**, *4*, 13.

adsorbate and the cationic position by theoretical means.<sup>2,6,34–40</sup> Nevertheless, a detailed picture of the cation position inside of zeolites and how this position affects the cation interaction with the probe molecules is still lacking.

Various probe molecules have been used to investigate the chemical nature of the cationic species: amines, nitriles, pyridines, and CO. Recently, Gorte<sup>41</sup> showed that strong bases, such as ammonia, are not a good probe for acidity measurements, because they are not specific to the Brønsted site. This means that some probe molecules can give distinct responses for qualitative and quantitative analysis of the site activity. Other probe molecules, such as methane and hydrogen, have been used as an alternative probe for cationic forms of zeolite.<sup>10,11,13</sup> Methane has a low adsorption affinity and has a close similarity to the molecules that are involved in current industrial processes, such as the aromatization of light hydrocarbons.

The present work systematically investigates the interaction of some probe molecules with Zn, loaded in different positions in chabazite. Applying periodic DFT at a molecular level, the adsorption energies of the probe molecules, the stability of the Zn cation in different sites, and the local distortions suffered by the framework have been studied.

## 2 Methods

In the work reported here, all calculations were performed using the Vienna ab initio Simulation Package (VASP).<sup>42,43</sup> This code carries out a periodic density functional calculations (DFT) using pseudopotentials and a plane-wave basis set. The DFT was parametrized in the local-density approximation (LDA), with the exchange-correlation

functional proposed by Perdew and Zunger<sup>44</sup> and corrected for nonlocality in the generalized gradient approximations (GGA) using Perdew-Wang 91 functional.<sup>45</sup>

The interaction between the core and electrons is described using the ultrasoft pseudopotentials (USPP) introduced by Vanderbilt<sup>46</sup> and provided by Kresse and Hafner.<sup>47</sup> These pseudopotentials allow a drastic reduction of the necessary number of plane waves per atom, especially for the first-row elements and for the third-row transition metals that exhibit contract 2p and 3d orbitals. The plane wave cutoff used here was 400.0 eV, which describes the oxygen atom better. Parameters such as k-points were kept fixed and equal to one ( $\gamma$ -point version of VASP). Forces, which are used to relax atoms into their equilibrium positions, can be easily calculated with VASP.

For the following reasons, the chabazite framework was chosen as a prototype of the zeolite. It contains only 12 TO<sub>2</sub> units per unit cell, which helps to save computational time required for calculations. Moreover, chabazites can be prepared using diverse Si/Al ratios and have micropores formed by eight-membered rings and cavities composed of four- and six-membered rings. These are large enough to host molecules such as ammonia, water, methanol, and C<sub>2</sub> to C<sub>4</sub> hydrocarbons (see Figure 1).

The original model consists of one unit cell of chabazite (rhombohedral cell,  $a = 9.389$ ,  $\alpha = 94.33^\circ$ ), as used previously by Jeanvoine et al.<sup>48</sup> and Sauer et al.<sup>49</sup> This unit cell was optimized at a constant volume using a quasi-Newton algorithm. The structural parameters were considered to be converged if the forces on the atoms became  $<0.05$  eV Å<sup>-1</sup>.

To reduce the problems related to the residual stress, which appear due to variations of the unit cell volume, the following procedure was used, which has been already applied with success in a similar study.<sup>50</sup> A set of configurations with varying fixed volumes within a small range of values close to the original value were optimized. These calculations generate a  $E$  (volume) curve. The equilibrium volume was determined via polynomial fit of this  $E$  (volume) curve, and structural parameters at a zero-pressure volume were taken. Finally, this new unit cell was further optimized.

Two unit cells have been used in some calculations, for instance, for the cation positions numbers 2, 3, and 4 (Figures 2, 3 and 4), to describe these positions better. The size consistency of the unit cell models has been tested, which produced equivalent results (within a few kJ/mol). Full optimization for all models has been conducted in this work.

Two aluminum atoms were placed into the chabazite framework, substituting two framework silicon atoms within the same unit cell, maintaining in all cases the ratio Si/Al = 5.0. Five symmetry nonequivalent configurations of aluminum atoms have been studied, obeying the Löwenstein's rule.<sup>51</sup> These configurations have also been previously studied theoretically by Grey et al.<sup>6</sup> using the Mott-Littleton crystal simulation method.

With respect to the relative aluminum distributions in the unit cell, seven different positions for the Brønsted site pair and for the zinc cation have been studied. The zinc cation substitutes the protons of the Brønsted sites in all models. The positions are shown in Figures 2, 3, and 4. Three different ring positions from the chabazite framework have been studied: 4T, 6T, and 8T ring. Two extra positions for the cation have also been analyzed: belonging to  $2 \times 4T$  rings (which corresponds to the  $\alpha$ -position described by Wichterlová),<sup>25</sup> and to  $2 \times 6T$  rings (which had been described by Grey et al.<sup>6</sup>). See Figure 4a,b, respectively.

Water and methane were used as probe molecules for the cationic site. Methane was used as a probe molecule in only four different

(22) Buckley, R. G.; Deckman, H. W.; Witzke, H.; McHenry, J. A. *J. Phys. Chem.* **1990**, *94*, 8384.

(23) Vitale, G.; Mellot, C. F.; Bull, L. M.; Cheetham, A. K. *J. Phys. Chem. B* **1997**, *101*, 4559.

(24) Huang, Y.; Paroli, R. M.; Delgado, A. H.; Richardson, T. A. *Spectrochim. Acta, Part A* **1988**, *54*, 1347.

(25) Sobalík, Z.; Tvaruzkova, Z.; Wichterlová, B. *J. Phys. Chem. B* **1998**, *102*, 1077.

(26) Channon, Y. M.; Catlow, C. R. A.; Jackson, R. A.; Owens, S. L. *Microporous Mesoporous Mater.* **1998**, *24*, 153.

(27) Wichterlová, B.; Dědčec, J.; Sobalík, Z. *Proceeds of the 12th International Zeolite Conference*; Treacy, M. M. J., Marcus, B. K., Bisher, M. E., Higgins, J. B., Eds.; Material Research Society: Baltimore, MD, 1999; p 941.

(28) Dědčec, J.; Kaucký, D.; Wichterlová, B. *Proceeds of the 12th International Zeolite Conference*; Treacy, M. M. J., Marcus, B. K., Bisher, M. E., Higgins, J. B., Eds.; Material Research Society: Baltimore, MD, 1999; p 1193.

(29) Savitz, S.; Siperstein, F. R.; Huber, R.; Tieri, S. M.; Gorte, R. J.; Myers, A. L.; Corbin, D. R. *J. Phys. Chem. B* **1999**, *103*, 8283.

(30) Dědčec, J.; Kaucký, D.; Wichterlová, B. *Microporous Mesoporous Mater.* **2000**, *35–36*, 483.

(31) Savitz, S.; Myers, A. L.; Gorte, R. J. *Microporous Mesoporous Mater.* **2000**, *37*, 33.

(32) Smith, L. J.; Eckert, H.; Cheetham, A. K. *J. Am. Chem. Soc.* **2000**, *122*, 1700.

(33) Turmes Palomino, G.; Bordiga, S.; Zecchina, A.; Marra, G.; Lanberti, C. *J. Phys. Chem. B* **2000**, *104*, 8641.

(34) Shubin, A. A.; Zhidomirov, G. M.; Yakovlev, A. L.; van Santen, R. A. *J. Phys. Chem.*, submitted.

(35) Yakovlev, A. L.; Shubin, A. A.; Zhidomirov, G. M.; van Santen, R. A. *Catal. Lett.*, submitted.

(36) Barbosa, L. A. M. M.; van Santen, R. A. *Catal. Lett.* **1999**, *63*, 97.

(37) Pierloot, K.; Delabie, A.; Ribbing, C.; Verberckmoes, A. A.; Shoeneydt, R. A. *J. Phys. Chem. B* **1998**, *102*, 10789.

(38) Su, B.-L.; Norberg, V.; Martens, J. A. *Microporous Mesoporous Mater.* **1998**, *25*, 151.

(39) Ferrari, A. M.; Neyman, K. M.; Huber, S.; Knözinger, H.; Röscher, N. *Lamguir* **1998**, *14*, 5559.

(40) Goursot, A.; Vasilyev, V.; Arbužnikov, A. *J. Phys. Chem. B* **1997**, *101*, 6420.

(41) Gorte, R. J. *Catal. Lett.* **1999**, *62*, 1.

(42) Kresse, G.; Furthmüller, J. *Comput. Mater. Sci.* **1996**, *6*, 15.

(43) Kresse, G.; Furthmüller, J. *Phys. Rev. B* **1996**, *54*, 169.

(44) Perdew, J.; Zunger, A. *Phys. Rev. B* **1981**, *23*, 8054.

(45) Perdew, J.; Wang, Y. *Phys. Rev. B* **1986**, *33*, 8800.

(46) Vanderbilt, D. *Phys. Rev. B* **1990**, *41*, 7892.

(47) Kresse, G.; Hafner, J. *J. Phys. Condens. Matter* **1994**, *6*, 8245.

(48) Jeanvoine, Y.; Ángyán, J. G.; Kresse, G.; Hafner, J. *J. Phys. Chem. B* **1998**, *102*, 7307.

(49) Brändle, M.; Sauer, J.; Dovesi, R.; Harrison, N. M. *J. Chem. Phys.* **1998**, *109*, 10379.

(50) Demuth, T.; Hafner, J.; Benco, L.; Toulhoat, H. *J. Phys. Chem. B* **2000**, *104*, 4593.

(51) Löwenstein, W. *Am. Mineral.* **1942**, *39*, 92.

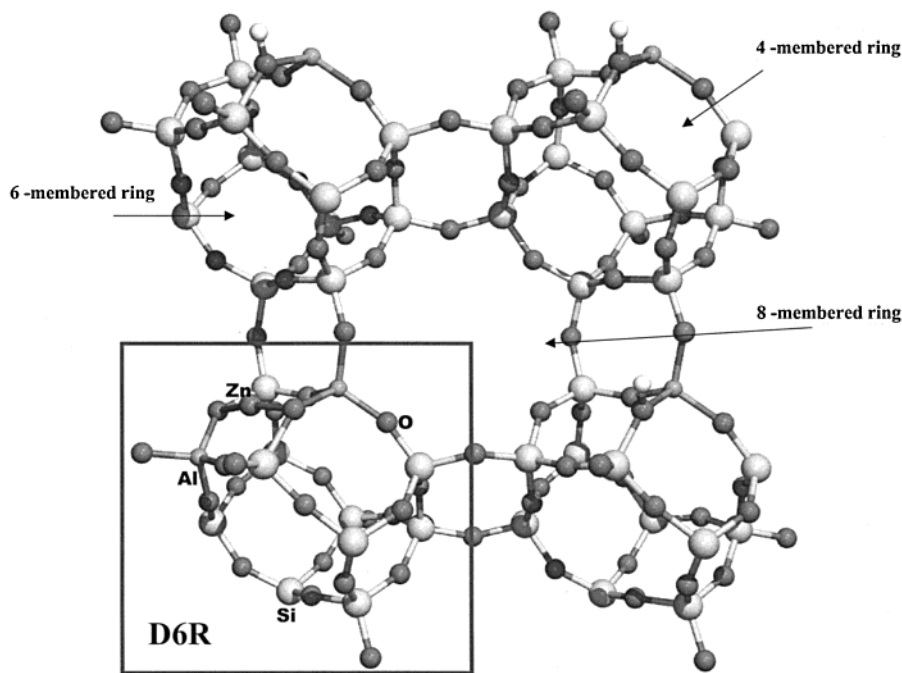


Figure 1. Chabazite structure with its unit cell.

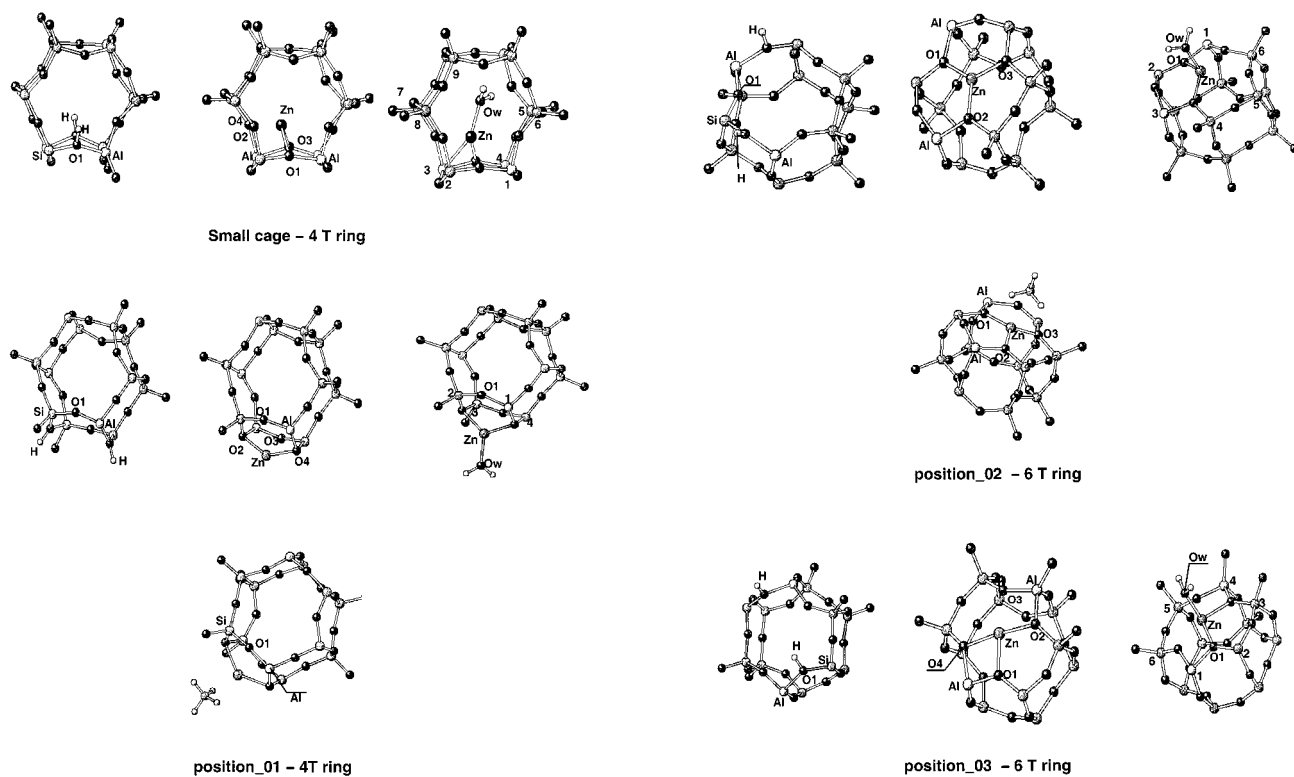


Figure 2. Four-membered ring configurations: small cage and position 01.

configurations: 4T, 6T (2 positions), and 8T rings. The reasons of these choices will be provided in the Discussion Section.

### 3 Results and Discussion

**3.1 The Preferred Location of Two Protons.** This study starts with a discussion of the siting of two aluminum atoms in the unit cell of chabazite. In the zeolite structure,  $\text{Si}^{4+}$  cations have been replaced by  $\text{Al}^{3+}$ . This substitution creates an excess of negative charge in the framework, which is compensated by addition of counteranions.<sup>52</sup> If such counteranions are protons,

Figure 3. Six-membered ring configurations: positions 02 and 03.

Brønsted sites are formed. Such sites are of great interest, because they are the key to the chemical behavior of solid acids.

The relative position of the aluminum atoms will influence the relative stability of the counteranions (protons), and consequently, the reactivity of the zeolite.

Seven different positions for the pair of aluminum atoms have been studied here, in combination with diverse types of framework rings. Protons have been placed either in the small cage, which is denoted by 4T ring (see Figure 2), or in the large

(52) van Santen, R. A.; Kramer, G. J. *Chem. Rev.* **1995**, *95*, 637.

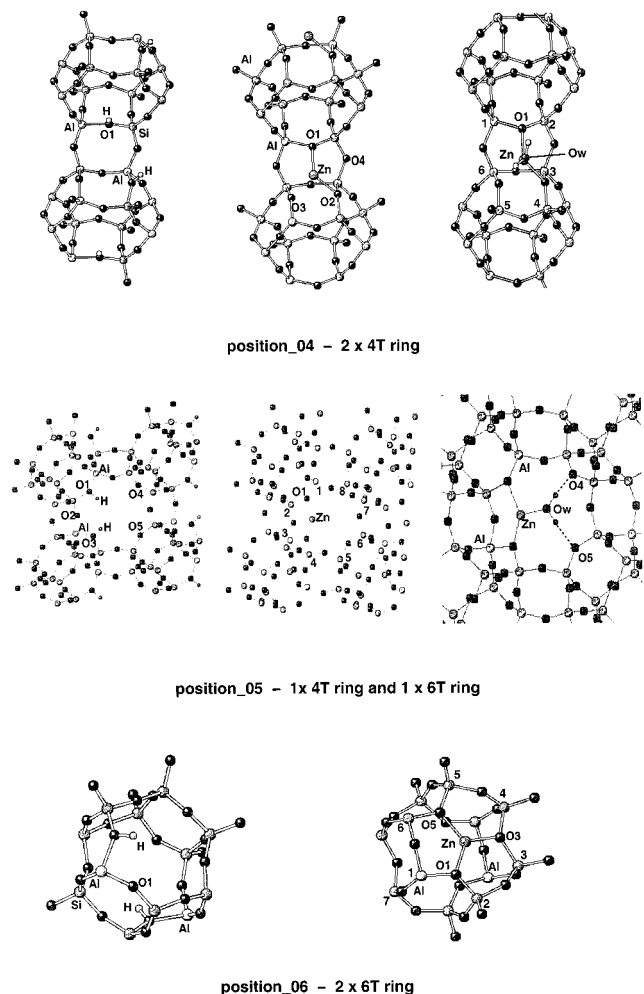


**Figure 4.** (a)  $2 \times$  four-membered and eight-membered ring configurations: positions 04 and 05. (b) The  $2 \times$  six-membered ring configuration: position 06.

cage, where the 6T and 8T rings are located (see Figures 3 and 4, respectively). In addition, two extra positions of protons have been studied: one proton in two different 4T rings (position 4) and one proton in two different 6T rings (position 6) (Figures 4a,b, respectively).

In Scheme 1, the relative stability of the pair of aluminum atoms in the chabazite models is shown. The 8T ring was chosen as a reference, because each aluminum atom of the Brønsted sites belongs to both six- and four-membered rings.

For all of the cases studied here, both of the protons prefer to bind in a small ring (4T ring), facing the large cage. This implies that the most reactive Brønsted site will be the six- or eight-membered rings, also facing the large cage. For MCM-22 zeolite, Sastre et al.<sup>53</sup> also established that stable and reactive Brønsted sites are mostly present in large rings.

Previously, Derouane et al.<sup>54</sup> had drawn similar conclusions using small basis set and Restricted Hartree–Fock (RHF) cluster calculations. They found that the two aluminum atoms preferred to be located in the small ring (4T) of mordenite.

Brändle et al.<sup>49</sup> studied proton siting in chabazite using a combined quantum mechanics/interatomic potential function (QM–Pot) method. They proposed that a single proton prefers

the 4T ring instead of the 6T ring. This proton position corresponds to position 01, as described in Figure 2.

Interestingly, positions 04 and 05 have two or one proton in 4T ring positions, respectively, which turns out to be more stable than both protons in the six-membered ring positions (compare positions 02, 03, 04, 05, and 06 in Scheme 1).

Position 03 is an exception. In this case, the two aluminum atoms have the largest separation in a six-membered ring. Although both Brønsted sites are located in the same ring, they behave as two independent Brønsted sites located in different 4T rings.

A detailed study of the siting of protons in the six-membered ring was performed. For positions 02 and 03, two different relative locations of protons were tested: position A is the nearest location of both protons, whereas in position B, the protons have the largest separation (see Scheme 2).

For position 02, the Brønsted sites prefer to be close to each other in OH–Al–O–Si pairs, similar to the 4T ring environment. Derouane et al.<sup>55</sup> had also described this interesting effect for the aluminum siting in zeolites. They calculated that even in larger rings, the aluminum atoms are more stable when both atoms are located in the same channel (or ring) in the Al–O–Si–O–Al sequence. This is also seen when one compares the stability of two Brønsted sites in positions 06 and 02 in Scheme 1. Position 02 (position 2A in Scheme 2), in which both Brønsted sites belong to the same six-membered ring, is about 21 kJ/mol more favorable.

For positions 04 and 05, there is only one silicon atom between the pair of aluminum atoms, again in a good agreement with the previous result from Derouane et al.<sup>55</sup>

Recently, Martucci et al.<sup>56</sup> studied the location of Brønsted sites in D-mordenites by neutron powder diffraction. They found four different positions for the Brønsted sites: one oxygen heading the side pocket, another toward the center of the 8T ring, and the last two pointing toward the center of the 12-membered ring. All of these positions also lead to the formation of the Al–O–Si–O–Al sequence.

The preference of this topological arrangement can be rationalized using the bond order conservation principle.<sup>57</sup> The weaker Al–O bond makes the neighboring bonds relatively stronger. The resulting alternations of the bond weakening and strengthening makes the second O–Al stronger (at position 02 B), which implies an attractive interaction.

For position 03, the location of the aluminum atoms leads to a large separation of the Brønsted sites. Position 03 B is more stable than position A by 19 kJ/mol (see Scheme 2).

**3.2 The Position of the Zn(II) Cation.** The Zn(II) stability is greatly influenced by the position of the original counter-cations (protons) in zeolite. Cation exchange is expected to be more favorable in positions where the protons are least stable. These should be located in the large rings.

Initially, the stability of Zn(II) was calculated from the reaction energy for the cationic exchange reaction (Scheme 3) and can be determined according to eq 1

$$\Delta E(\text{exchange})_{(\text{position } n)} = E(\text{Zn model})_{(\text{position } n)} - E(\text{H model})_{(\text{position } n)} \quad (1)$$

In Scheme 4, this energy for the Zn(II) cation at different

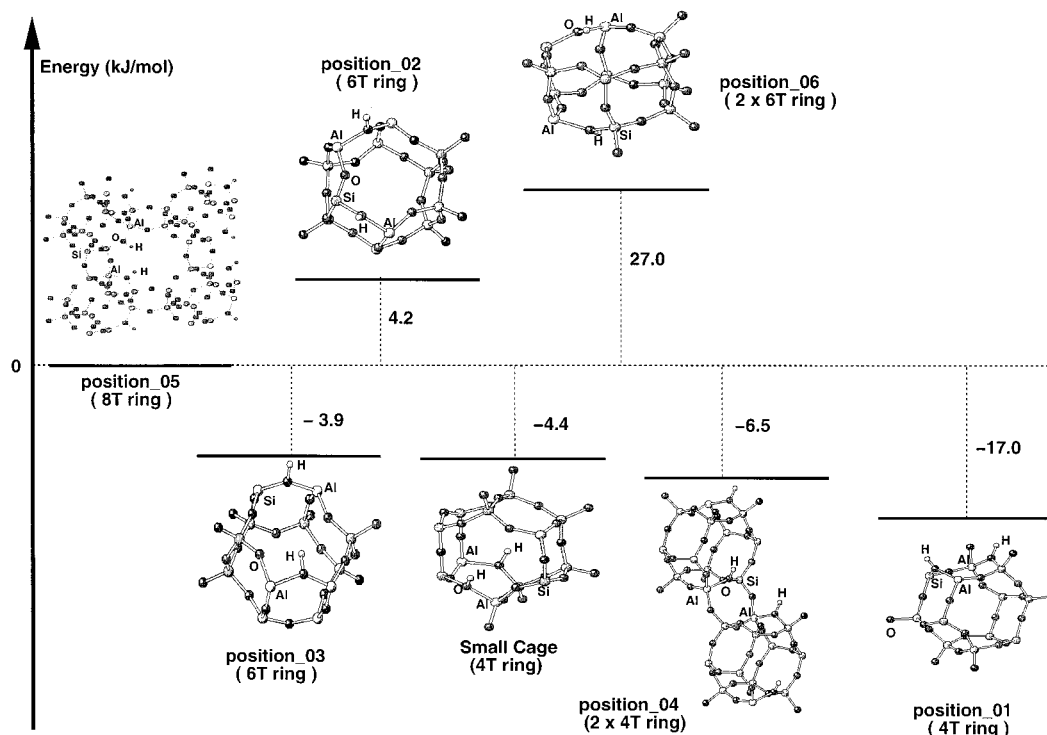
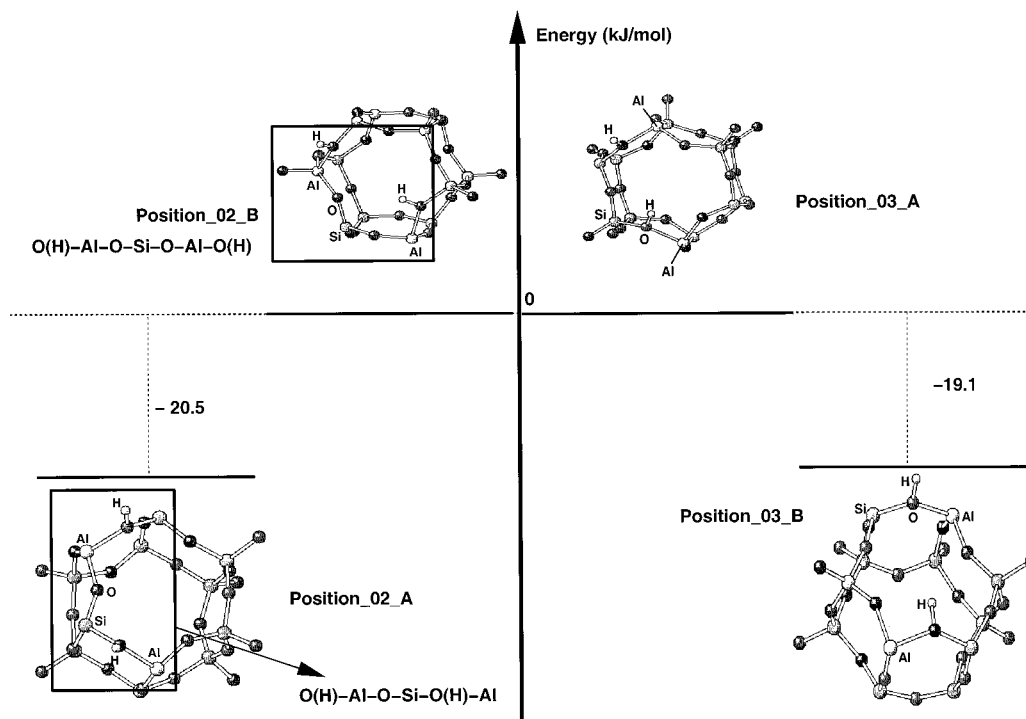
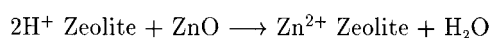
(55) Derouane, E. G.; Fripiat, J. G. *Zeolites* **1985**, *5*, 165.

(56) Martucci, A.; Cruciani, G.; Alberti, A.; Ritter, C.; Ciambelli, P.; Rapacciuolo, M. *Microporous Mesoporous Mater.* **2000**, *35–36*, 405.

(57) van Santen, R. A. *Theoretical Heterogeneous Catalysis; World Scientific Lecture and Course Notes in Chemistry 5*; World Scientific: Singapore, 1991; pp 204, 291.

(53) Sastre, G.; Fornes, V.; Corma, A. *J. Phys. Chem. B* **2000**, *104*, 4349.

(54) Derouane, E. G.; Fripiat, J. G. *Proceeds of the 6th International Zeolite Conference*, Reno, NV, 1983.

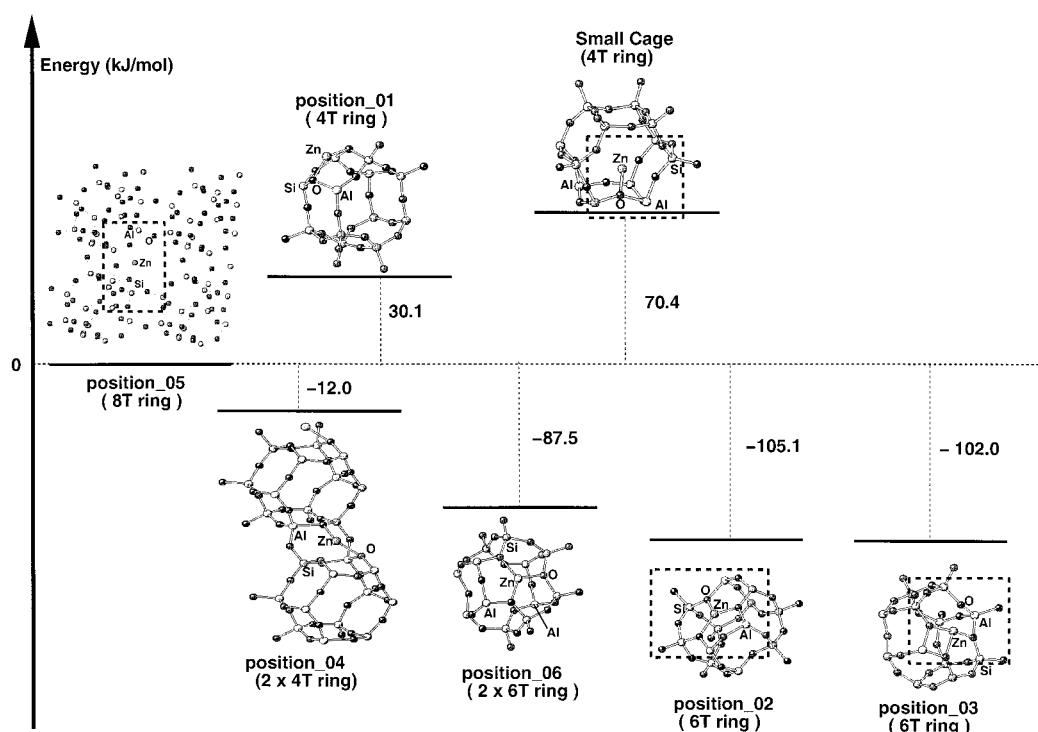
**Scheme 1.** Relative Stability of Two Brønsted Sites Placed in Different Rings**Scheme 2.** Stability of Two Brønsted Sites Placed in the Different Six-Membered Ring Configurations**Scheme 3.** Cation Exchange Reaction Model

positions is plotted. Once more, the 8T ring was used as a reference. The positions in which Zn cation sites are in large rings (see positions 02, 03, and 06) are the most stable.

Positions 02 and 03 have similar cationic exchange energy. This result does not, however, indicate the most stable configuration. To identify this cationic position, a simple comparison of the absolute energy of positions 02 and 03

$[E(\text{Zn model})_{(\text{position } n)}]$  is made, and it shows that position 03 is 5 kJ/mol more stable.

This slightly higher stability of position 03 arises as a consequence of the distortions that occur in the six-membered ring. For instance, in this configuration, the T–O–T angle distortions are not large, reaching a maximum value of  $10^\circ$  in modulus (see Table 1). In position 02, such T–O–T angle distortions, however, have a wider range: from 5 to  $24^\circ$  in modulus. Such T–O–T angle distortions in the six-membered rings with this aluminum distribution have previously been

**Scheme 4.** Relative Exchange Energy of the Zn<sup>2+</sup> Cation for the Different Positions**Table 1.** Results for the Optimized Geometry for the Different Six-Membered Rings<sup>a</sup>

	zeolite			
	H	Zn	Zn-water	Zn-methane
Position 02				
T1-O-T2	145.0	126.0	146.5	124.8
T2-O-T3	135.5	140.9	139.1	140.1
T3-O-T4	147.5	123.6	120.8	124.5
T4-O-T5	148.0	144.9	146.9	144.7
T5-O-T6	151.5	128.5	152.3	127.5
T6-O-T1	136.2	147.8	135.3	147.2
Zn-O1		1.90	2.03	1.91
Zn-O2		1.93	2.02	1.94
Zn-O3		2.00	2.83	2.02
Zn-O(w)			2.07	
d(O1-O2-Zn-O3)		-175.4	-134.0	-145.7
Position 03				
T1-O-T2	139.0	131.2	131.3	129.8
T2-O-T3	151.1	141.4	142.5	139.8
T3-O-T4	142.7	127.2	130.9	126.6
T4-O-T5	136.0	132.9	134.2	134.2
T5-O-T6	160.7	159.4	159.6	162.2
T6-O-T1	141.1	131.5	135.6	133.1
Zn-O1		2.08	2.09	2.07
Zn-O2		2.01	2.08	2.04
Zn-O3		2.17	2.21	2.17
Zn-O4		2.07	2.14	2.12
Zn-O(w)			2.09	
d(O1-O2-Zn-O4)		-175.9	-163.62	-168.4

<sup>a</sup> Distances are in Å and angles, in degrees.

found in cluster calculations<sup>58</sup> and experimentally by FTIR investigations in Y zeolites.<sup>59</sup>

Cationic positions 02 and 03 have also been found previously by others. Vitale et al.<sup>60</sup> studied the position of Ca<sup>2+</sup> in LSX by

(58) Delabie, A.; Pierloot, K.; Groothaert, M. H.; Weckhuysse, B. M.; Schoonheydt, R. A. *Microporous Mesoporous Mater.* **2000**, *37*, 209.

(59) Jacobs, W. P. J. H.; van Wolput, J. H. M. C.; van Santen, R. A. *Zeolites* **1993**, *13*, 170.

(60) Vitale, G.; Bull, L. M.; Morris, R. E.; Cheetam, A. K.; Toby, B. H.; Coe, C. G.; MacDougall, J. E. *J. Phys. Chem.* **1995**, *99*, 16087.

X-ray and neutron diffraction. Calcium cations are located preferentially at sites I and II. The latter site, which corresponds to the center of the six-membered ring, interacts strongly with deuterated benzene. Using molecular dynamics, Gulians et al.<sup>61</sup> found a similar result for Cu<sup>2+</sup> in mordenite, in which the cation also sits above the six-membered ring.

Recently, Grey et al.<sup>6</sup> studied the location of the Ca(II) cation in chabazite by the Mott-Littleton method. They showed that the most strongly bound site is always the cationic position above the six-membered ring. The most stable situation is equal to position 03 calculated here, in which the six-membered ring has two aluminum atoms at opposite sides. The second most stable situation is equal to position 02, and the energy difference between them is about 10 kJ/mol, which is in agreement with the results presented here.

Another interesting result is the stability of the cation in position 06. Even though the Zn cation position is virtually the same as in position 02, the exchange energy is distinct. There are two counteracting effects that control the cation stability in this position. First, the T-O-T angle distortions after cation exchange are very large for position 06, for which the resulting energy cost would make this position unstable, see Table 2. The magnitude of the distortions that occur in the six-membered ring seems to depend on the local Si/Al ratio (see positions 02 and 06 in Figures 03 and 04b, respectively). Similar results have also been found in cluster calculations.<sup>37</sup>

The second effect is charge compensation, which depends on the distribution of aluminum atoms in the framework. In position 02, the cation has only two aluminum atoms in a sphere of about 6 Å of radius, centered in the Zn(II) cation. This is not the case for position 06, in which there are three aluminum atoms inside the sphere of the same radius (see Figure 5). This relationship between the cationic position and the aluminum atom distribution in the zeolite framework has also been noticed in the theoretical investigation of cation substitution in heu-

(61) Gulians, V. V.; Mullhaupt, J. T.; Newsam, J. M.; Gorman, A. M.; Freeman, C. M. *Catal. Today* **1999**, *50*, 661.

**Table 2.** Results for the Optimized Geometry of the Extra Studied Positions<sup>a</sup>

	zeolite			
	H	Zn	Zn-water	Zn-methane
Position 04 (2 × 4T rings)				
T1-O-T2	134.2	128.7	128.6	
T2-O-T3	153.5	136.0	134.1	
T3-O-T4	132.7	128.9	129.8	
T4-O-T5	157.9	145.1	142.8	
T5-O-T6	138.2	133.7	134.5	
T6-O-T1	155.2	137.0	137.4	
T6-O-T3	143.8	154.8	148.3	
O2-O3	3.61	3.02	2.97	
Zn-O1		1.97	2.02	
Zn-O2		2.00	2.03	
Zn-O3		2.11	2.16	
Zn-O(w)			2.03	
d (T1-T3-T6-O2)	105.9	98.9	99.0	
Position 05 8T ring (1 × 4T ring, 1 × 6T ring)				
T1-O-T2	136.8	125.2	128.5	127.7
T2-O-T3	140.2	141.9	143.9	146.6
T3-O-T4	128.6	115.8	119.7	118.7
T4-O-T5	145.9	145.5	147.6	146.5
T5-O-T6	148.5	147.2	138.0	146.3
T6-O-T7	146.4	145.5	146.0	148.7
T7-O-T8	151.7	149.7	137.3	149.0
T8-O-T1	141.9	144.9	146.4	146.6
Zn-O1		2.00	2.16	2.09
Zn-O(2)		2.06	2.03	2.06
Zn-O3		1.94	2.06	1.98
Zn-O(w)			1.92	
H(w)-O4			1.75	
H(w)-O5			1.87	
Position 06 (2 × 6T ring)				
T1-O-T2	153.6	125.4		
T2-O-T3	143.3	147.6		
T3-O-T4	158.5	127.7		
T4-O-T5	148.4	149.4		
T5-O-T6	158.6	127.0		
T6-O-T1	138.3	143.0		
T1-O-T7	142.3	142.5		
T7-O-T8	161.5	136.0		
T8-O-T9	137.8	137.5		
T9-O-T10	155.3	132.3		
Zn-O1		1.90		
Zn-O3		1.98		
Zn-O5		1.95		

<sup>a</sup> Distances are in Å and angles, in degrees.

landint-type zeolites.<sup>26</sup> This electronic effect seems to compensate partially for the energy loss due to the distortions in the T-O-T angles, which occur after cation exchange.

The framework distortions play an important role in the cation stability among the six-membered rings, as shown before. This framework flexibility has been noticed previously in different zeolite studies. Štich et al.<sup>62</sup> suggested that the framework elasticity may significantly lower the energy barrier for the methanol activation. A similar relation was indicated for the formation of the hydronium cation in gmelinite.<sup>63</sup> Recently, Smith et al.<sup>64</sup> showed that the increase of the length of the unit cell of chabazite drives some changes of its framework to form a perfect arrangement for the Na<sup>+</sup> cation occupation at site II (six-membered ring), which is in good agreement with the results presented here.

(62) Štich, I.; Gale, J. D.; Terakuna, K.; Payne, M. C. *J. Am. Chem. Soc.* **1999**, *121*, 3292.

(63) Benco, L.; Demuth, Th.; Hafner, J.; Hutschka, F. *Chem. Phys. Lett.* **2000**, *324*, 373.

(64) Smith, L. J.; Eckert, H.; Cheetham, A. K. *J. Am. Chem. Soc.* **2000**, *122*, 1700.

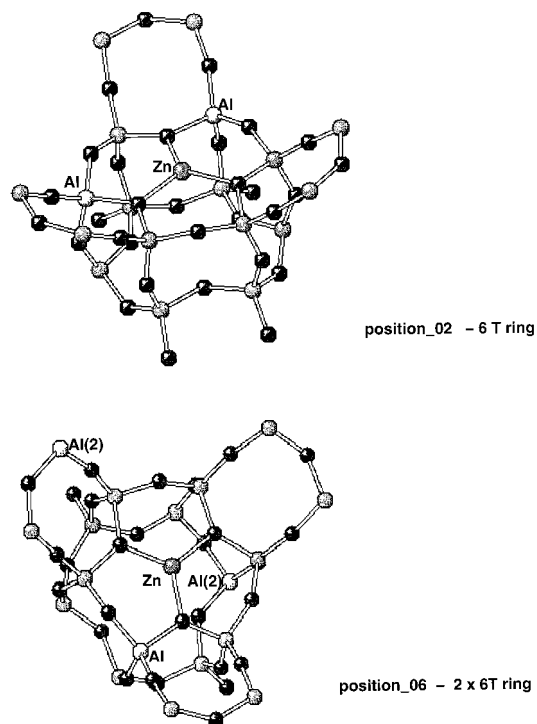


**Figure 5.** Aluminum distribution near the Zn active site: positions 02 and 06.

Hammonds et al.<sup>65</sup> showed that zeolites, whose frameworks are not infinitely flexible, can achieve the necessary distortions of their structures without deformation of the SiO<sub>4</sub> and AlO<sub>4</sub> tetrahedra; hence, it costs very little energy. This is possible due to the existence of some low-energy deformation modes in the zeolite structure, which are determined by the balance between the number of degrees of freedom of the structural components (SiO<sub>4</sub> and AlO<sub>4</sub> tetrahedra) and the constraints introduced by linking these components. If one takes into account that symmetry can make some of the constraints for aluminosilicates to be redundant, the latter balance has a positive value for zeolites, and thus, enables some zeolite framework modes to distort, with some entropy gain.

They identified, for instance, one such mode for faujasite. It gives rise to a distortion of the framework about site II, which corresponds to the six-membered. This is in good agreement with the results found for positions 03 and 02.

Position 04 behaves as two 4T rings for proton siting. This situation changes for the Zn cation, which stabilizes as a six-membered ring. The association of the two 4T rings can also be identified as a six-membered ring with an oxygen bridge that links the T3 atom to the T6 atom (see Figure 4). The Zn(II) cation is bound to oxygen atoms O1 and O2, with the distances equal to 1.97 and 2.00 Å, respectively. These distances are in good agreement with the calculated Zn-O distances for Zn in position 02, which is a “true” six-membered ring.

Vitale et al.<sup>23</sup> studied the position of the Na cation in NaX zeolite by neutron diffraction and Monte Carlo simulations. The Na cation prefers to occupy position III', which is similar to the position 04 studied here.

Protons are the most stable in position 01, in which the oxygen atoms face the large cage. Thus, this position is expected to be less favorable for exchange with a cation, as compared to the position in the small cage. Interestingly, this is not found in

(65) Hammonds, K. D.; Deng, H.; Heine, V.; Dove, M. T. *Phys. Rev. Lett.* **1997**, *78*, 3701.

**Table 3.** Results for the Optimized Geometry for the Different four-membered Rings<sup>a</sup>

	zeolite			
	H	Zn	Zn-water	Zn-methane
	Small Cage			
T1-O-T2	135.1	167.5	170.0	
T2-O-T3	136.9	128.7	127.5	
T3-O-T4	131.9	145.9	158.9	
T4-O-T1	146.3	132.6	135.0	
T1-O-T6	148.0	146.5	142.7	
T4-O-T5	155.3	147.8	146.2	
T2-O-T7	170.7	150.3	158.9	
T3-O-T8	169.1	161.3	161.5	
T2-T9	5.35	5.55	5.63	
Zn-O1		2.16	2.13	
Zn-O2		2.10	2.24	
Zn-O3		1.96	2.01	
Zn-O4		2.30	2.34	
Zn-O(w)			1.87	
	Position 01			
T1-O-T2	160.0	168.8	151.8	171.3
T2-O-T3	130.2	128.7	131.0	132.2
T3-O-T4	174.2	164.8	155.9	162.0
T4-O-T1	127.0	128.0	130.4	129.1
Zn-O1		2.16	2.90	2.33
Zn-O2		1.96	1.94	2.01
Zn-O3		2.25	2.32	2.16
Zn-O4		1.96	1.97	2.01
Zn-O(w)			1.98	

<sup>a</sup> Distances are in Å and angles, in degrees.

the calculations. This is due to significant distortions in the double 6-ring cage (D6R) that appears after cation exchange in the small cage position (see the T2-O-T7 and T3-O-T8 angles and the T2-T9 distance in Table 3). Most probably these distortions cannot be compensated for by some entropy gain, as discussed earlier for the six-membered ring. This indicates that these low-energy deformation modes may be connected to the AlO<sub>4</sub> tetrahedron content and distribution in the zeolite framework.

The cations in these 4T ring positions are the most reactive, although the Zn cation is exposed to molecules only at position 01. Goursot et al.<sup>40</sup> studied the adsorption of N<sub>2</sub> and CO to NaX zeolites. These calculations showed that the initial absorption of the molecules occurred at the 4T ring position (position III).

Simulation studies of *p*-xylene isomer on KY zeolite<sup>66</sup> and of HFC-134 and HFC-134A on X and Y zeolites<sup>29</sup> also indicate that site III in the 4T ring is very reactive. In the case of xylene adsorption, this molecule changes its adsorption configuration to position II as a result of the presence of an extra cation in position III. In the other case, the selectivity in the separation process is higher in the Y zeolites as a result of the presence of the cation in the 4T ring positions.

Experimentally, the cationic site in natural chabazite has been investigated by Calligaris et al.<sup>16,18</sup> In both of these studies, four different sites were found: I, near the center of the 6T ring; II, along the [111] direction near the center of the large cavity; III, in the center of the D6R cage; and IV, near the 8T ring aperture. Site II was found only in hydrated samples for Mn<sup>2+</sup>/chabazite. Site I corresponds to positions 02 and 03 according to our notation. Site IV corresponds to position 05. Position 04 (Figure 4a) can also be assigned to the latter site, although the cation is not completely in the plane of the 8T ring. After

dehydration of the sample, remarkable deformations are reported in all of these sites, in very good agreement with the results found in the calculations.

Experimental site III was not considered stable in the calculations, because the cation prefers to locate in the six-membered ring (position 06 in Scheme 1), in which there is a high aluminum concentration.

In experimental studies of the cationic position in chabazite<sup>16,18</sup> the Si/Al ratio is 2, indicating the presence of a higher aluminum content. Moreover, the cation lies in the center of the D6R unit only under special conditions:<sup>6</sup> namely, when the aluminum atoms are not in the same six-membered ring or, in the case where there are no aluminum atoms present, in the D6R cage.

Cheetham et al.<sup>32</sup> located the cationic sites in Li,Na-chabazite in a recent study using a combination of solid-state NMR and neutron powder diffraction. Lithium prefers both the six- and the four-ring windows, but the introduction of sodium into Li-chabazite reduces the occupation, primarily at the four-ring site and then the six-ring site. This is in good agreement with the results found here.

Wichterlová et al.<sup>27,28,30</sup> have studied the siting and coordination of cations in zeolites by diffuse reflectance spectroscopy in the visible region. They also identified in ferrierite, ZSM5, and mordenite three different cationic positions: position  $\alpha$  (site E according to Mortier et al.<sup>67</sup>) is situated in the main channel, and position  $\beta$  (site A<sup>67</sup>) is near the eight and six rings of mordenite, ZSM5, or ferrierite. The third position, so-called  $\gamma$  (site C<sup>67</sup>), is in a boat-shaped site. They suggested that Co and Cu ions are strongly bound to the framework in the  $\gamma$ -position, inducing a large local perturbation of the adjacent T-O-T angle. The  $\gamma$ -site occupation is low.

The cations are weakly bound in the  $\alpha$ -site, thus inducing smaller perturbation of the T-O-T angles. This position was found to exhibit the highest activity in the selective catalytic reduction (SCR) of NO by methane. Position  $\beta$  is the most populated for both Co and Cu in ZSM5 and ferrierite. Cations in this position are less active than in the  $\alpha$ -position.

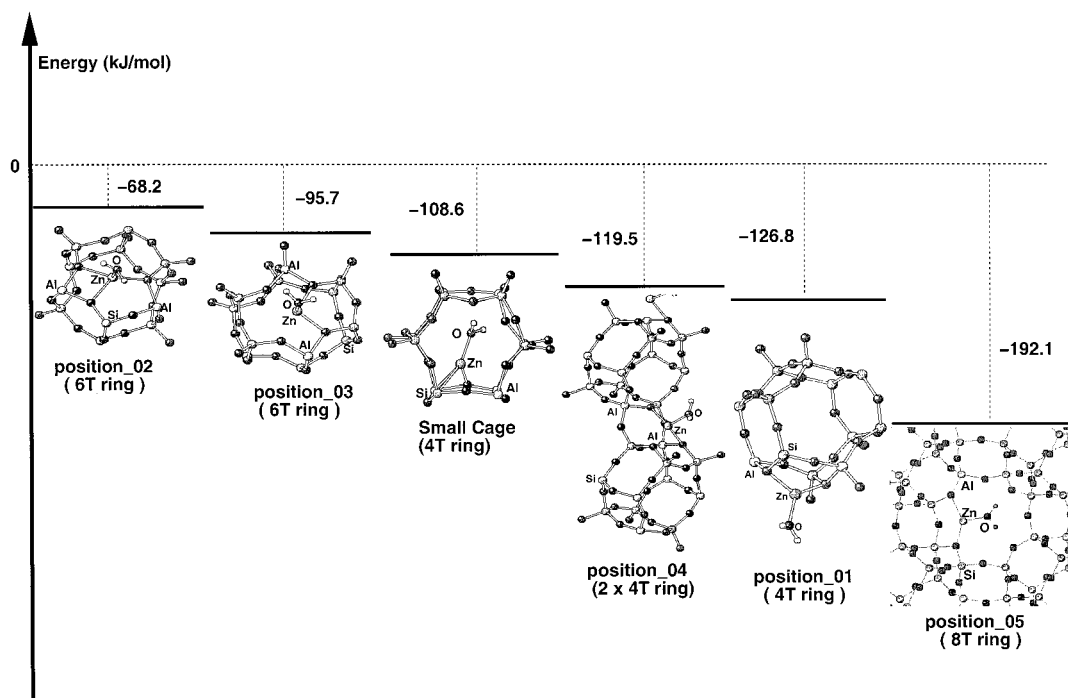
These three different cationic positions can be identified with the positions studied here. For instance, positions 02, 03, and 06 of this paper can be identified with the  $\beta$ -position. They are the most stable positions for the Zn(II) cation; therefore, they can be expected to be the most populated. They would also be less reactive than positions 01, 04, and 05, which can be correlated to the  $\alpha$ -position. The deformations suffered in the latter positions (01, 04, and 05) are very small as compared to the one suffered in the small cage position (see Tables 1 and 2), which most likely corresponds to the  $\gamma$ -position. The small cage position is the least stable position for Zn(II); thus, it should be more reactive. This result does not agree completely with the description of the  $\gamma$ -site by Wichterlová et al.<sup>27</sup> This may be due to the difference in the aluminum content or the distribution of aluminum atoms.

Raman spectroscopy, which also provides vibrational information, often in a complementary manner to infrared spectroscopy, has been studied previously by several authors.<sup>19,20,22,24</sup> In these works, the T-O-T vibration has been analyzed in the region between 300 and 600 cm<sup>-1</sup>.<sup>19,20</sup> There are some significant changes in the vibrational spectrum of Na<sup>+</sup> replaced by Li<sup>+</sup> in zeolite A. The latter cation tends to distort the zeolite structure because of its strong polarizability and great tendency toward coordination, whereas Na<sup>+</sup> does not. This result is in

(66) Lachet, V.; Boutin, A.; Tavitián, B.; Fuchs, A. H. *Langmuir* **1999**, *15*, 8678.

(67) Mortier, W. J. *Compilation of Extraframework Sites in Zeolites*; Butterworth Co. Ltd.: Guilford, U.K., 1982.



**Scheme 5.** Adsorption Energy of the Water Molecule in the Different Cationic Sites

agreement with the results found here, where Zn at higher coordination (position 03) induces more distortions in the zeolite framework.

Low frequencies in the region of 40–340  $\text{cm}^{-1}$ , which indicates the cation vibration, have also been used to identify the cationic position.<sup>68</sup> The band at 135  $\text{cm}^{-1}$  represented the cation at site II (six-membered ring) for KY zeolite, and at 195  $\text{cm}^{-1}$ , the sodium cation at the same site for NaY zeolite. In both cases, the cationic-preferred position was again identified to be in the six-membered ring.

**3.3 The Adsorption of Probe Molecules.** The cationic positions described in the previous section have been probed by interacting with a water molecule. The adsorption energy of the water molecule is shown in Scheme 5.

The results calculated for positions 01 and 04 follow the inverse trend of the cation stability: the less stable the cationic position, the higher the adsorption energy. The small cage position, however, has a lower value than the latter positions for the water adsorption energy. If one compares the distance [Zn–O(w)] between the Zn(II) cation and the oxygen atom from the water molecule (see Tables 2, 3), one finds that water binds stronger to the Zn(II) cation in a small cage position;  $\text{Zn}-\text{O}(\text{w})_{\text{small}} > \text{Zn}-\text{O}(\text{w})_{01} > \text{Zn}-\text{O}(\text{w})_{04}$ . This unexpected result for the small cage position is due to the deformations that occur in the D6R cage after the adsorption of water. The D6R cage has to accommodate the steric constraints, which appear as a result of interaction with the water molecule. The T2–O–T7 and T3–O–T8 angles increase, as well as the distance between T2 and T9 (see Table 3 and Figure 2).

For positions 04 and 05, the distance [Zn–O(w)] is in agreement with the stability trend (see Tables 2, 3). Position 01, however, does not comply with it. Although the framework does not change significantly for both cases (positions 01 and 05), the shorter distance [Zn–O(w)] shows stronger interaction with the Zn(II) cation in position 05. The water molecule pulls

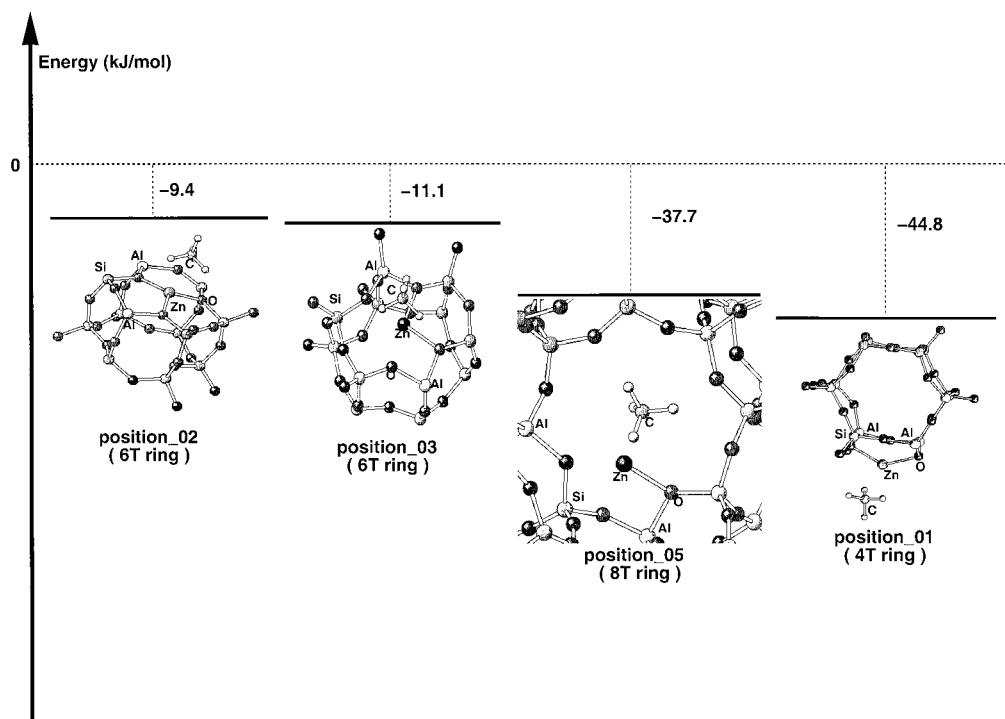
off the cation in position 05 from its original position, weakening the bonds Zn–O1 and Zn–O3 (see Table 2). The alternating weakening and strengthening of bond lengths that occurs in the eight-membered rings as a consequence of the bond order conservation principle make the O4–Si bond weak. This O4 atom, then, creates a hydrogen bond with the water molecule (see the H(w)–O4 distance in Table 2), highly stabilizing the system.

The lowest adsorption energy values are found for positions 02 and 03, in agreement to the cation stability trend. These values are unexpected, however, because the Zn cation is slightly more stable at position 03 than at the other one. The explanation for such behavior is related to the interaction of the cation with the probe molecule itself. The water molecule binds in the same way in both cases (see the value for Zn–O(w) in Table 1). The system zeolite plus cation, however, is strongly perturbed by this interaction. The cation is extracted from its original position by the water molecule (see the dihedral angle between the oxygen atoms of the ring and the cation, Table 1). The framework relaxes its structure to compensate for this change. Interestingly, the T–O–T angles return in most of the cases to the initial values (compare these values for H– and Zn–water models, Table 1). Although the extraction is more pronounced in the case of position 02, the relaxation of the ring is better noticed for position 03. This result shows again that a highly symmetric position of aluminum atoms for six-membered rings brings more stability to the system, at least in chabazite. Moreover, the adsorption energy of position 03 is very close to the one found for the small-cage position, confirming the distinct influence of the framework distortion.

This effect of cationic migration is well-known in the literature. Klier<sup>21</sup> mentioned that a CO molecule induces Cu(I) movement from less accessible to more accessible positions in type-Y zeolites. This effect has also been noticed for ZSM5, in which CO modifies the coordination geometry of the Cu(I) cation.<sup>69</sup> Su et al.<sup>38</sup> proposed that the  $\text{Na}^+$  cation also migrates from the sodalite cages and hexagonal prisms in NaEMT under

(68) Jacobs, W. P. J. H.; van Wolput, J. H. M. C.; van Santen, R. A. *Zeolites* **1992**, 12, 315.

(69) Sárkány, J. *App. Catal. A* **1999**, 188, 369.

**Scheme 6.** Adsorption Energy of Methane in the Different Cationic Sites

the influence of a benzene molecule. Wichterlová<sup>25</sup> showed by FTIR measurements that ammonia perturbs  $\text{Mn}^{2+}$ ,  $\text{Co}^{2+}$ ,  $\text{Mg}^{2+}$ , and  $\text{Ni}^{2+}$  dehydrated ferrierites, removing the cation from its original position. Buckley et al.<sup>22</sup> also noticed such sorbate perturbations using Raman spectroscopy. In potassium-ZK5 zeolite, they verified that eight- and six-membered rings exhibit some structural deformations with increasing water loading.

To investigate this effect further, another probe molecule, methane, was chosen. Methane has no dipole moment and interacts weakly with the cation, which means that the lattice relaxations are expected to be small. Four different cationic positions were chosen: 02, in which the cation is severely extracted from its original position by the water molecule; 03; 05; and 01, which is one of the least stable locations for the Zn(II) cation. The results are plotted in Scheme 6.

As expected, in contrast with strongly adsorbing  $\text{H}_2\text{O}$ , the adsorption energy of methane follows the cationic stability trend. The cation in position 01 interacts more strongly with the new probe molecule than do those in the other positions. The methane molecule is unable to form hydrogen bonds with the framework oxygen, as the water molecule does; therefore, the adsorption energy calculated for position 05 has a lower value than it does for position 01.

The cation moves slightly away from its original position in the case of positions 02 and 03, but the ring structure remains almost intact and, consequently, the adsorption energies for both positions are very similar (see Table 1). These results mean that different probe molecules can give quite distinct responses for qualitative and quantitative analysis of the site activity.

Recently, Khelifa et al.<sup>70</sup> studied the sorption of  $\text{CO}_2$  by zeolite X exchanged with  $\text{Zn}^{2+}$ . They reported that for a high degree of Zn cation exchange, the appearance of Zn(II) in the supercages leads to a strong  $\text{Zn}^{2+}$  cation–sorbate interaction. This is in agreement with our findings. The sites S(III) and S(III'), which correspond to the cationic position in the small

four-membered ring, are most populated at a higher degree of cation exchange.

An interesting result is found for the methane adsorption configuration at position 05. The methane interacts with the cation with  $C_{3v}$  symmetry at the four- and six-membered ring,<sup>71</sup> but with the cation with  $C_{2v}$  symmetry at the eight-membered ring.

#### 4 Conclusions

The siting of  $\text{Zn}^{2+}$  cations in the Zn-exchanged zeolite has been studied by the periodical density functional method. Chabazite was selected as a zeolite prototype model, because it contains the four-, six-, and eight-membered rings commonly found in zeolite structures. Two aluminum atoms have been employed to substitute for the silicon atoms in the same unit cell of the zeolite framework. Different preferred arrangements are found for the Brønsted site pair and the Zn(II) cation.

The two Brønsted sites are more stable when placed in the small ring (4T ring) than in the other rings. As a consequence, the most reactive Brønsted sites are located in large rings. These two Brønsted sites prefer to be arranged according to the  $\text{O}(\text{H})\text{—Al—O—Si—O}(\text{H})\text{—Al}$  sequence in the same ring, instead of being located in two different rings.

The Zn(II) cation stability is markedly influenced by framework distortions. Other factors that also contribute to the stabilization are the aluminum concentration near the cation and the relative stability of the original Brønsted sites. The  $\text{Zn}^{2+}$  cation is more stable in the larger rings. The six-membered one is the most stable configuration. As a consequence, in the small rings, the cation is expected to be more reactive.

Interaction with probe molecules can also significantly influence the zeolite structure. When probe molecules interact strongly with the active center, the cation can be extracted from its original position. In the case of the water molecule, this effect leads to a high framework relaxation. This, however, does not

(70) Khelifa, A.; Derriche, Z.; Bengueddach, A. *Microporous Mesoporous Mater.* **1999**, *32*, 199.

(71) Barbosa, L. A. M. M.; Zhidomirov, G. M.; van Santen, R. A. *Phys. Chem. Chem. Phys.* **2000**, *17*, 3909.

occur for methane, which is weakly bound to the active site. The analysis of the activity and reactivity of the cations exchanged in zeolites, obtained by the adsorption of a probe molecule, should be done carefully, because the binding energy of a probe molecule is strongly influenced by framework relaxation and the cationic position environment.

**Acknowledgment.** L.A.M.M. Barbosa thanks the National Council of Scientific and Technologic Development (CNPq, Brazil) and Eindhoven University of Technology (TUE, The Netherlands) for financial support.

JA002175E